Azulene-based compounds for targeting orexin receptors

Teppo O. Leino[a,#,], Ainoleena Turku[a,b,#], Jari Yli-Kauhaluoma[a], Jyrki P. Kukkonen[b,c], Henri Xhaard[a] and Erik A. A. Wallén[a]*

[a] Drug Research Program, Division of Pharmaceutical Chemistry and Technology, Faculty of Pharmacy, University of Helsinki, P.O. Box 56, FI-00014 University of Helsinki, Finland

[b] Department of Veterinary Biosciences, Faculty of Veterinary Medicine, University of Helsinki, P.O. Box 66, FI-00014 University of Helsinki, Finland

[c] Department of Physiology, Faculty of Medicine, University of Helsinki, P.O. Box 63, FI-00014 University of Helsinki, Finland

[*] Corresponding author, e-mail: teppo.leino@helsinki.fi

[#] Equal contribution

ABSTRACT

A library of 70 000 synthetically accessible azulene-based compounds was virtually screened at the OX_2 receptor. Based on the results, a series of azulene derivatives was synthesized and the binding to and activation of both orexin receptor subtypes were assessed. Two most promising binders were determined to have inhibition constants in the 3–9 μM range and two other compounds showed weak OX_2 receptor agonism. Furthermore, three compounds exhibited a concentration-dependent potentiation of the response to orexin-A at the OX_1 but not the OX_2 receptors. Altogether this data opens new approaches for further development of antagonists, agonists, and potentiators of orexin response based on the azulene scaffold.

KEYWORDS

Azulene, orexin receptor, potentiator, agonist, antagonist, sleep-wake regulation

ABBREVIATIONS

BINAP, 2,2'-bis(diphenylphosphino)-1,1'-binaphthyl; CHO, Chinese hamster ovary (cells); dppf, 1,1′-bis(diphenylphosphino)ferrocene; EDC, 1-ethyl-3-(3-dimethylaminopropyl)carbodiimide; HBM, HEPES-buffered medium; HOBt, 1-hydroxybenzotriazole; NIS, *N*-iodosuccinimide.

1 INTRODUCTION

The orexin (hypocretin) system, comprising the two G protein-coupled orexin receptors OX_1 and OX_2 and the agonistic neuropeptides orexin-A and orexin-B, plays a key role in sleep-wake regulation.[1–3] In addition to arousal, the orexin system has been reported to affect metabolism, nociception, addiction, and stress response.[4] The orexin system has primarily been targeted in sleep-promoting pharmacotherapies, resulting in a large number of orexin receptor antagonists developed for insomnia.[3,5] Orexin receptor agonists, however, have received less attention, and only a few small molecular agonists have been reported.[6–10] In the CNS, orexin receptor agonists might prove useful in the treatment of daytime sleepiness, especially in narcolepsy.[11] Activating orexin receptors in periphery would have other therapeutic indications, such as cancer.[12] Small molecular potentiators that enhance the effects of endogenous orexin-A have also been reported.[13] These potentiators would have application as orexin receptor activation therapies when production of the endogenous peptides is not fully terminated.

In our efforts to target orexin receptors, we decided to explore azulene-based compounds postulating that the lipophilic azulene ring could be integrated into a peptide mimetic of the amphipatic α-helical C-terminus of orexin-A.[21,22] A supporting observation was that multiple aromatic rings are found in known orexin receptor ligands, usually as biaryls or fused bicyclic aryls.[3] Azulene is an interesting scaffold in medicinal chemistry as it resembles several other bicyclic aromatics that are frequently found in drugs. Azulene, a structural isomer of naphthalene, is a bicyclic nonbenzenoid aromatic hydrocarbon having a dipole moment due to the electron-rich five-membered ring and electron-deficient seven-membered ring.[14] Therefore, it bears resemblance also to indole. In medicinal chemistry, azulene is an unexplored scaffold; only one azulene-based drug, the antiulcer agent egualen sodium, is currently on the market.[15] In addition, there are a few other published examples of azulenes with application as anticancer [16–18] and antidiabetic [19] agents and in erectile dysfunction.[20]

The study was initiated by developing general synthetic protocols to access 1,3,6-trisubstituted azulenes.[21,22] These positions are on different edges of the azulene ring and reach a large space around the central scaffold. In addition, the positions 1 and 3 are the most reactive sites on the azulene ring, and substituting these positions is therefore beneficial for the stability of the end products. Furthermore, the substitution at the 6-position yields symmetrical synthesis intermediates. This facilitates the further substitution of 1- and 3-positions, namely by avoiding selectivity issues during the synthesis. As the developed synthetic routes make thousands of compounds accessible, we employed a docking-based virtual screening to prioritize the compounds to be synthesized.

2 RESULTS AND DISCUSSION

2.1 Selecting compounds for synthesis. To prioritize compounds for synthesis, we first constructed a virtual library of di- and trisubstituted azulenes using the combinatorial database

building tool of Schrödinger Maestro 2015v3.[23] We selected a pool of substituents presenting diverse physicochemical properties and size; we also included substituents that are found in already published agonists/antagonists of the orexin receptors. These substituents vary in their hydrogen-bonding properties, size, aromaticity, and the lengths of linkers between the substituents and the azulene scaffold. The substituents placed in the compounds actually synthesized was driven in part by our expectation that a particular combination would be synthetically accessible. The initial pool of substituents at the 1- and 3-positions was composed of the same 63 functional groups; the whole pool was used at the 1-position, while at the 3-position, after considering the viability of the resulting combinations, we used 46 substituents (of which 45 are directly a subset of the initial pool; Supporting Information Figure S1). At the 6-position the initial pool was composed for one half of the subset of substituents used for 1-position and for the other half of a new set of polar/charged substituents. As a result, a virtual library containing 70 038 azulene-based compounds of molecular weight under 500 g/mol was constructed.

We then docked this virtual library to the three-dimensional structure of the OX_2 receptor [24] using the software Glide from the Schrödinger Maestro 2015v3 package.[23] The docking was conducted under the assumption of binding at the site of the co-crystallized antagonist. A shortlist of compounds was constructed among the 200 top-scoring docking poses that interacted with Gln134[3.32] (for nomenclature see references [25,26]) and preferably also with Tyr317[6.48]. These interactions are present in the used OX_2 crystal structure,[24] and suggested to take place upon binding of the endogenous peptide orexin-A.[27]

The favorable interactions with Gln134[3.32] and Tyr317[6.48] were frequently formed by compounds with unsubstituted or 4-trifluoromethyl-substituted benzoyl groups at the 1-position, hydrogen atoms or unsubstituted and 4-methoxy-substituted benzoyl groups at the 3-position, and amide or carboxyl groups at the 6-position. We thus prioritized compounds with these substituents for synthesis. The functional groups outlined to make favorable interactions with Gln134[3.32] and Tyr317[6.48] are among the preferred substituents but not necessarily ranked first; when we studied the substituent distribution in the top-scoring 5% of the docked database (7200 poses; Supporting Information Figures S2 and S3), the benzoyl and 4-(trifluoromethyl)benzoyl groups ranked 6th and 15th in the 1-position, hydrogen atom and benzoyl group ranked 7th and 33rd in the 3-position, and primary carboxamide, and the corresponding carboxyl group ranked 1st and 6th in the 6-position. This is explainable by the compounds being assessed as a whole by the docking program. In total, we decided to synthesize 16 compounds from the shortlist, and to test them together with eight previously synthesized compounds [22] and seven synthetic intermediates.

2.2 Synthesis. We used 6-methylazulene (**1**) as the starting material to synthesize the designed compounds employing formylation, iodination, Suzuki cross-coupling and the modified Vilsmeier–Haack reactions in the functionalization of the five-membered ring of azulene, as described before.[21] Additionally, we have previously demonstrated conversion of the methyl group at the 6-position to other functionalities, either via a formyl group, or via a methyl anion. This methodology was developed further in this study as described below.

3

We investigated oxidation of 6-formylazulene (**2**) to obtain the ester **4**. Since our attempts to synthesize **4** directly from **2** with a method originally developed for benzaldehydes failed,[28] we oxidized **2** with Oxone to give 6-carboxyazulene (**3**) in 48% yield (Scheme 1). The reaction did not go to completion as 32% of the starting material was recovered. Extension of the reaction time did not improve the yield, although the starting material was now consumed almost completely. Nevertheless, the ester **4** was obtained after treating **3** with iodomethane in the presence of base.
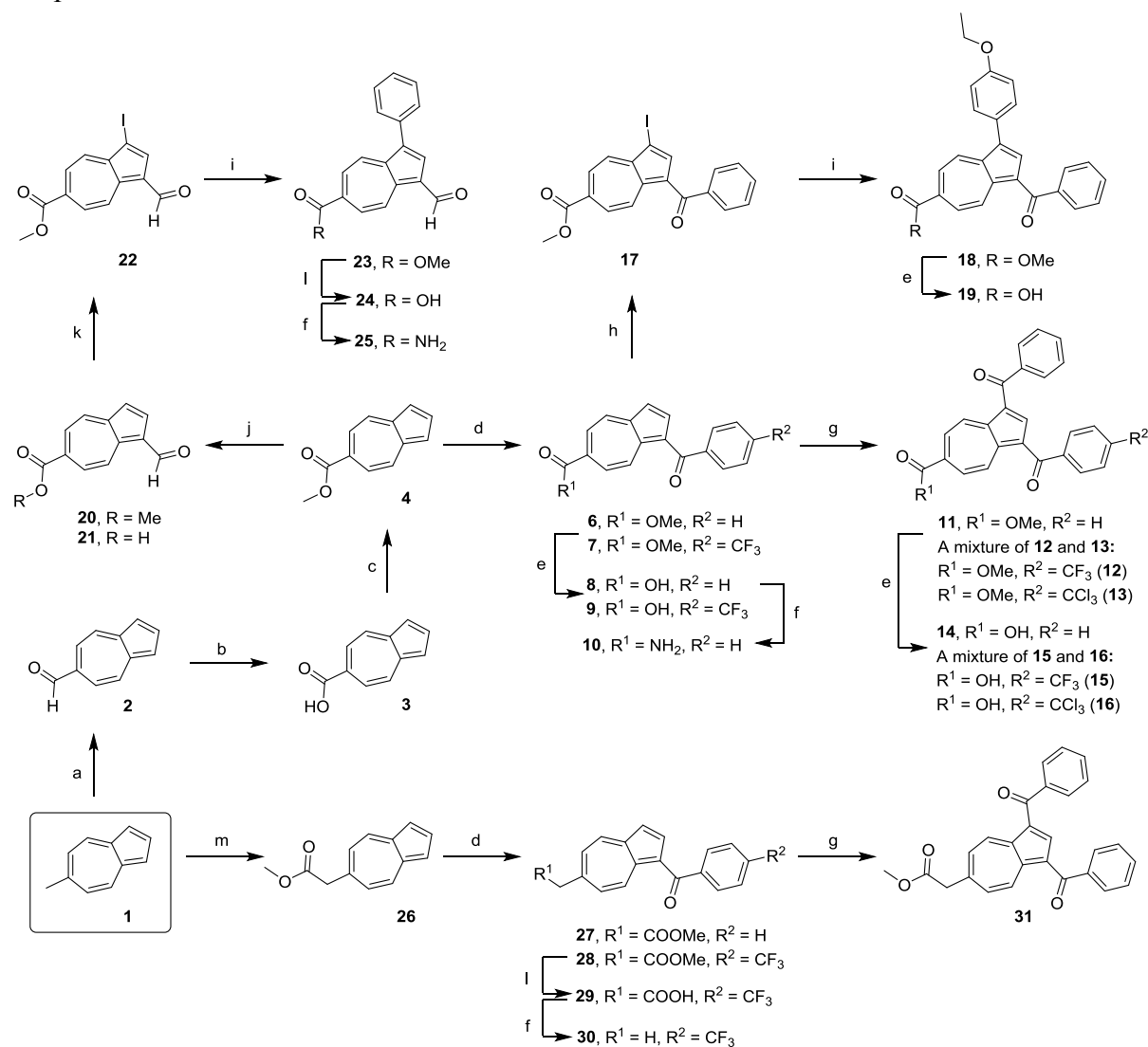
Scheme 1. Synthesis of designed azulene-based compounds. Reagents and conditions: (a) see ref.[21] (b) Oxone, DMF, rt, 3 h, 48%; (c) K_2CO_3, iodomethane, DMF, rt, 45 min, 96%; (d) An appropriate *N,N*-dimethylbenzamide, $POCl_3$, 1,4-dioxane, mw, 100 °C, 3–5 h, 63% (**6**), 75% (**7**), 39% (**27**), 43% (**28**); (e) NaOH, H_2O, MeOH, THF, rt, 0.5–28 h, 82% (**8**), 87% (**9**), 34% (**14**), 6% (**19**); (f) i) EDC·HCl, HOBt·H_2O, DMF, 0 °C, 15 min, rt, 1 h, ii) NH_3 (aq), rt, 2.5–4 h, 87% (**10**), 35% (**25**), 85% (**30**) (g) Benzoyl chloride, $AlCl_3$, DCM, 0 °C, 30 min, rt, 4–23 h, 87% (**11**), 73% (**31**); (h) NIS, DCM, 0 °C, 30 min, rt, 3.5 h, 98%; (i) An appropriate phenylboronic acid, Pd(dppf)Cl_2, BINAP, Cs_2CO_3, toluene, mw, 110 °C, 1 h, 84% (**18**), 88% (**23**); (j) (Chloromethylene)dimethyliminium chloride, DCM, 0 °C, 1 h, 61% (**20**), 15% (**21**); (k) NIS, DCM, 0 °C, 1.5 h, rt, 19 h, 98%; (l) NaOH, H_2O, THF, rt, 2 h, 92% (**24**), 78% (**29**);

(m) i) LDA, THF, 0 °C, 10 min, rt, 20 min, ii) Methyl chloroformate, −78 °C, 10 min, −78 °C → 0 °C, 45 min, 52%.

Since we did not succeed in adding the second benzoyl group to the five-membered ring of **6** under the modified Vilsmeier–Haack conditions, we used a Friedel–Crafts acylation instead to obtain **11** in 87% yield (Scheme 1). Applying the same Friedel–Crafts conditions for compound **7** led to a mixture of **12** and **13** in low yield. These two compounds were not separable from each other despite several attempts by flash chromatography.

Additionally, we noticed that the carboxylic acid **29** is prone to decarboxylation and we failed in converting it to the corresponding primary amide. Only the decarboxylated product **30** was obtained in 85% yield.

Compounds **32–39** have been synthesized with another route developed for 1-acyloxyazulene derivatives, and their synthetic procedures have been described in detail previously.[22]

2.3 Binding and Ca^{2+} elevation. We first screened compounds **6–25** and **27–39** using a competition binding assay in Chinese hamster ovary-K1 (CHO) cells heterologously expressing high densities of human OX$_1$ and OX$_2$ receptors.[29,30] The binding of each compound was measured at a single concentration, 10 μM, in competition with 1 nM [^{125}I]-orexin-A (see Experimental Section). As a result, twelve compounds (**8**, **20–22**, **30**, **32–38**) showed clear (>30%) and statistically significant inhibition of [^{125}I]-orexin-A binding to either or both receptor subtypes (Table 1, Figure 1A). Unexpectedly, six compounds (**7**, **9**, **17**, **19**, **27**, and **28**) significantly increased the binding of [^{125}I]-orexin-A to the OX$_1$ receptors and to a lesser extend to the OX$_2$ receptors (i.e. the % inhibition is negative in Table 1; filled circles in Figure 1A). This effect will be discussed in more detail below (see **2.4 Potentiation of orexin-A binding and Ca^{2+} response**).

Then, we determined the inhibitory constants for the two most promising compounds using a Ca^{2+} elevation assay (Supporting Information Figure S4). Compound **22** had K_i values of 4.8 and 3.6 μM and **32** had K_i values 7.6 and 8.6 μM, for the OX$_1$ and OX$_2$ receptors, respectively (Table 1). It should be noted that concentrations only up to 10 μM were used for curve-fitting, which prevented the responses to reach a plateau. This was due to avoid over-estimations at high compound concentrations (due e.g. to aggregation). The reported affinities are thus not absolute and therefore should be considered as apparent K_i values.

Table 1. Inhibition of [^{125}I]-orexin-A binding at 10 μM concentration (% inhibition) and K_i values of **19**, **22** and **32** as determined upon competition with orexin-A in the Ca^{2+} assay (μM). Data are shown as averages of values determined in 3–4 independent experiments in quadruplicate. *: $P < 0.05$.
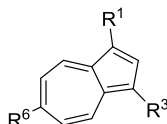
Compound	R¹	R³	R⁶	Inhibition of [¹²⁵I]-orexin-A binding (at 10 μM compound concentration; %), and K_i (μM; shown in parentheses)	
				OX₁	OX₂
22	(aldehyde, CHO)	(I)	(methyl ester, CO₂Me)	40.7 ± 13.0% * (4.8 ± 1.8 μM)	47.2 ± 6.8% * (3.6 ± 1.1 μM)
32	(acetate ester, OC(O)CH₃)	(CH₂-morpholine)	(Cl)	24.5 ± 10.7% * (7.6 ± 2.0 μM)	46.7 ± 10.7% * (8.6 ± 2.8 μM)
21	(aldehyde, CHO)	(H)	(carboxylic acid, CO₂H)	37.8 ± 6.0% *	44.1 ± 9.5% *
33	(acetate ester, OC(O)CH₃)	(aldehyde, CHO)	(vinyl-imidazole)	23.0 ± 4.8% *	39.9 ± 7.1% *
20	(aldehyde, CHO)	(H)	(methyl ester, CO₂Me)	25.0 ± 9.7% *	37.2 ± 11.1% *
34	(Boc-glycine ester)	(H)	(Cl)	−4.5 ± 2.5% *	36.0 ± 7.6% *
35	(benzyl carbonate)	(H)	(Cl)	18.2 ± 2.8% *	35.6 ± 4.1% *
36	(benzoate ester)	(H)	(Cl)	0.1 ± 12.9%	34.3 ± 9.1% *
37	(thiophene-2-carboxylate ester)	(H)	(Cl)	9.8 ± 10.8%	33.2 ± 10.2% *
8	(benzoyl, PhC=O)	(H)	(carboxylic acid, CO₂H)	11.0 ± 16.5%	32.9 ± 12.0% *
38	(nicotinate ester)	(H)	(Cl)	−2.4 ± 12.5%	32.3 ± 9.2% *
30	(4-CF₃-benzoyl)	(H)	(Me)	38.3 ± 0.8% *	31.0 ± 15.6%
6	(benzoyl, PhC=O)	(H)	(methyl ester, CO₂Me)	7.2 ± 17.2%	28.9 ± 8.5% *
14	(benzoyl, PhC=O)	(benzoyl, PhC=O)	(carboxylic acid, CO₂H)	−10.4 ± 6.1%	27.0 ± 12.5%
A 47:53 mixture of 12 and 13	(12: 4-CF₃-benzoyl; 13: 4-CCl₃-benzoyl)	(benzoyl, PhC=O)	(methyl ester, CO₂Me)	18.3 ± 8.5% *	26.4 ± 7.8% *
A 47:53 mixture of 15 and 16	(15: 4-CF₃-benzoyl; 16: 4-CCl₃-benzoyl)	(benzoyl, PhC=O)	(carboxylic acid, CO₂H)	19.9 ± 11.3% *	25.6 ± 8.8% *
39	(methyl succinate ester)	(H)	(Cl)	8.0 ± 7.0%	24.3 ± 4.2% *

6

#					
24				16.2 ± 8.1% *	21.5 ± 10.1% *
18				8.4 ± 12.3%	19.1 ± 9.6%
10				13.6 ± 10.5%	18.0 ± 13.9%
25				6.1 ± 8.5%	16.7 ± 11.8%
29				8.6 ± 13.3%	11.2 ± 10.4%
23				8.5 ± 8.9%	1.8 ± 3.4%
9				−81.5 ± 18.6% *	1.0 ± 5.8%
28				−30.4 ± 10.6% *	1.0 ± 3.6%
27				−37.7 ± 8.1% *	−4.3 ± 18.7%
17				−34.9 ± 2.1% *	−5.4 ± 8.2%
11				−10.6 ± 16.1 %	−14.5 ± 12.4 %
19				−24.0 ± 4.8% * (7.5 ± 0.9 μM)	−16.9 ± 16.4% (4.9 ± 2.0 μM)
31				−21.4 ± 11.9%	−20.4 ± 11.2%
7				−60.5 ± 19.8% *	−47.4 ± 11.4% *

In addition, we screened the compounds **6–25** and **27–39** for the agonist activity in a Ca^{2+} elevation assay at 10 μM concentration (Figure 1B). In the screening, compounds **6**, **7** and **27** caused a Ca^{2+} elevation of 5–12% of the maximum response (E_{max}) to orexin-A at both receptor subtypes, while the other compounds did not cause notable Ca^{2+} elevation. Since the observed Ca^{2+} elevation is not necessarily due to orexin receptor agonism, we tested compounds **6**, **7** and **27** also in control CHO-K1 cells (not expressing orexin receptors). In the OX_2-expressing cells, the responses to **7** and **27** were approximately 5 %-units higher than those in the control cells (Figure 1C). We confirmed this observation by assessing the Ca^{2+} responses to **7** and **27** in the presence of an excess of known orexin receptor antagonists, the OX_1-selective **41** (SB-334867) and OX_2-selective **42** (TCS-1102), in OX_1- and OX_2-expressing cells, respectively (for structures of **41** and **42**, see Supporting Information Figure S5). The orexin receptor-specific responses, i.e. the response above the control cell response and the response suppressed by the antagonist, were fully in line (data not shown). Altogether, this suggests compounds **7** and **27** to act as weak OX_2 receptor agonists. The Ca^{2+} responses to **7** and **27** at the OX_1 receptors and

6 at both orexin receptor subtypes were of similar magnitude as those of control cells, and thus these responses appeared nonspecific (Figure 1C).
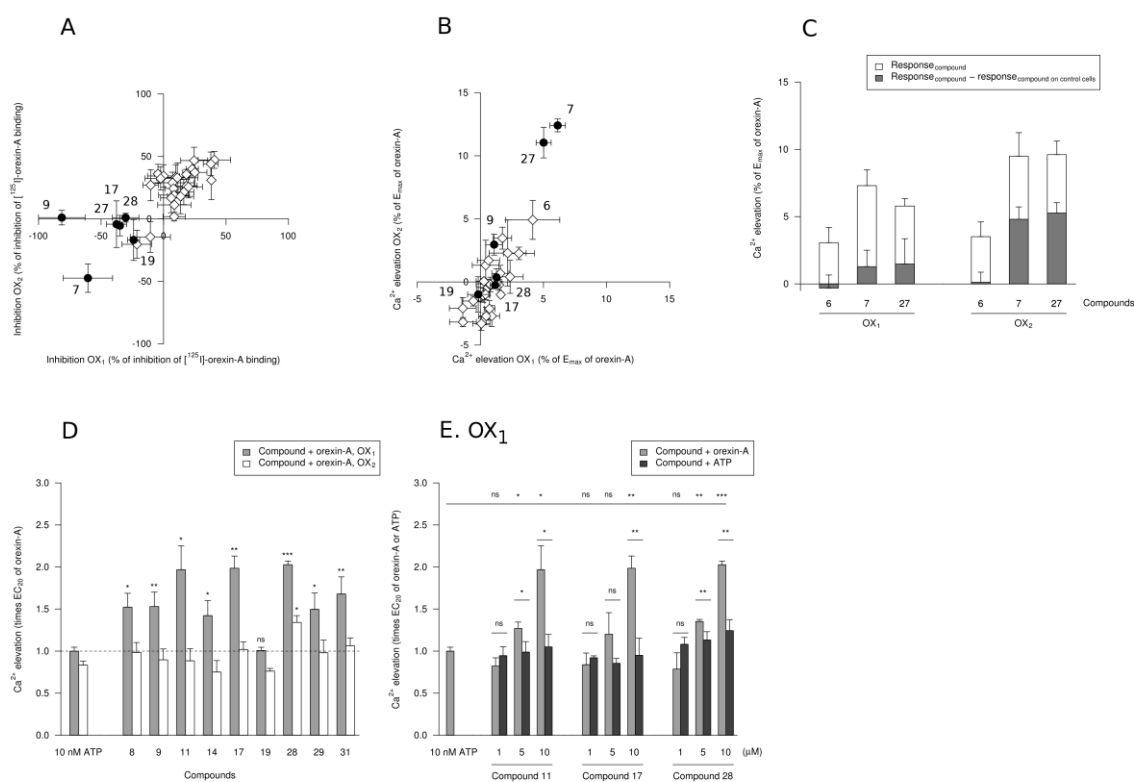
Figure 1. **A.** Inhibition of $[^{125}I]$-orexin-A binding screened with all of the compounds at 10 µM concentration, n=3−4. **B.** Screening of Ca^{2+} responses of all compounds at 10 µM concentration given as a percentage of E_{max} of orexin-A, n=2. In A and B, compounds which enhance $[^{125}I]$-orexin-A binding significantly (i.e. give negative inhibition values) are marked as filled circles. **C.** Total Ca^{2+} responses and specific (orexin receptor-mediated; assessed utilizing control CHO cells) Ca^{2+} responses of the three compounds, which displayed highest Ca^{2+} response in the screening. The responses were normalized to the E_{max} of orexin-A separately before averaging. n=3−4 **D.** The effects of the compounds at 10 µM concentration on the orexin-A response in the Ca^{2+} elevation assay. **E.** The effects of three most promising OX_1 receptor potentiators on the Ca^{2+} responses elicited by 0.02–0.03 nM orexin-A and 60 nM ATP (corresponding to the EC_{20} of each ligand; see the text for the details). The responses were separately normalized to the control orexin-A or ATP response, respectively, for each independent experiment before averaging. The significances were calculated for the Ca^{2+} responses as compared with the corresponding control. ns (not significant) $P > 0.05$, $*P < 0.05$, $**P < 0.01$, $***P < 0.001$; n = 3−4.

2.4 Potentiation of orexin-A binding and Ca^{2+} response. Potentiation of the actions of orexin-A is the outcome of several interconnected processes and is difficult to apprehend as a whole. Such a potentiation may combine allosteric actions both intra-receptor and through

dimers or oligomers, formation of a ternary receptor–orexin-A–potentiator complex, and indirect effect through extracellular and intracellular Ca^{2+} levels or activation of downstream signaling machinery.[30–34]

In particular, orexin-A binding displays self-potentiation (positive cooperativity),[30] and we have observed a similar effect with small molecular ligands as well.[9] Here, compounds **7**, **9**, **17**, **19**, **27** and **28** promoted [^{125}I]-orexin-A binding. This effect is characterized by concentration-response curves with a bell-shaped initial response, i.e. [^{125}I]-orexin-A binding initially increases before being reduced at higher concentrations of unlabeled orexin-A or a small molecular competitor. Since we screened the binding at a single concentration (Table 1, Figure 1A), there is no indication that, for example, compound **9** (binding assay values –81.5 ± 18.6% on OX_1 and 1.0 ± 5.8% on OX_2) would potentiate [^{125}I]-orexin-A binding more effectively than **7** (–60.5 ± 19.8% on OX_1 and –47.4 ± 11.4% on OX_2), because these data points can be either from the ascending or the descending part of their concentration-response curves.

Given that the orexin-A peptide occupies a single site at each receptor, the self-potentiation of orexin-A binding most likely occurs through receptor dimers or oligomers. An important correlate is that if small molecules are able to potentiate orexin-A binding in the same way, they also likely bind to the orthosteric binding site. This allows us to reconcile the diverse pharmacology observed (antagonists, weak agonists, potentiators) under the parsimonious idea that azulene-based compounds all dock to the same binding site. Yet, because the potentiating effect of orexin-A binding occurs only at low orexin-A concentrations, i.e. at low receptor occupancy, it is not the major factor in the observed potentiation of Ca^{2+} elevation (described below).

The other factor to consider is calcium, both extracellular and intracellular. Binding of the orexin-A peptide requires extracellular Ca^{2+}, as suggested by the decrease of [^{125}I]-orexin-A binding when extracellular Ca^{2+} levels are reduced.[30] Whether increasing the intracellular Ca^{2+} levels would potentiate orexin-A binding has, however, not been studied previously. Here, compounds **7** and **27** caused an intracellular Ca^{2+} elevation at both OX_1- and OX_2-expressing cells, which could play a role in the potentiation of [^{125}I]-orexin-A binding if Ca^{2+} efflux would occur (Table 1; Figure 1A–B). However, agonism does not offer any explanation in the case of compounds **9**, **17**, **19**, and **28** that do not elevate cytosolic Ca^{2+}. Another possible mechanism of the potentiation of the actions of orexin-A by intracellular Ca^{2+} is the activation of the downstream molecular machinery.[30–34]

We decided to study further the compounds, which potentiated orexin-A binding. Thus, we assessed the Ca^{2+} responses of the compounds **7**, **9**, **17**, **19**, **27** and **28** in a presence of 0.02–0.03 nM orexin-A; the orexin-A concentration was separately adjusted in each bath of the cells to approximately correspond the EC_{20} of the orexin-A. We expanded the pool of tested compounds to **6**, **8**, **11**, **14**, **29** and **31** that potentiated the binding of orexin-A to OX_1 receptors on some of the individual experiments (data not shown). Because changes in the intracellular Ca^{2+} levels might potentiate the response to orexin-A, we used controls that mimicked the effect of the compounds on the intracellular Ca^{2+}. For compounds **8**, **9**, **11**, **14**, **17**, **19**, **28**, **29** and **31**, which did not trigger Ca^{2+} elevation, we used 10 nM ATP as a control; this ATP

concentration does not cause a detectable Ca^{2+} elevation by itself. For **6**, **7** and **27**, we used 30 nM ATP as a control, since this concentration of ATP elevates the intracellular Ca^{2+} levels to the same magnitude as the Ca^{2+} responses to these compounds.

As a result, with the exception of **19**, all tested compounds potentiated the Ca^{2+} response to orexin-A by at least 1.4-fold on OX_1 receptors at 10 µM concentration (Figure 1D, Supporting Information Figure S6). Interestingly, the potentiation effect was specific to the OX_1 receptors, except for compound **28** that showed a weak potentiation at the OX_2 receptors too (Figure 1D). The potentiating effects of compounds **8**, **9**, **11**, **14**, **17**, **28**, **29** and **31** were significantly higher than that of the control (10 nM ATP; Figure 1D). The potentiation of the Ca^{2+} response to orexin-A induced by compounds **6**, **7** and **27**, instead, was not significantly different from that of 30 nM ATP (Supporting Information Figure S6). This might indicate that the compound-mediated increase of the intracellular Ca^{2+} levels potentiated the orexin-A response, not these compounds *per se*. It may also be that the Ca^{2+} elevation triggered by these compounds makes the detection of potentiation effects too challenging. Altogether, out of the four compounds that promoted $[^{125}I]$-orexin-A binding at the concentration tested, three (**9**, **17** and **28** but not **19**) were found to be able to significantly promote orexin-A mediated Ca^{2+} elevation. Furthermore, all five additional compounds tested (**8**, **11**, **14**, **29** and **31**) potentiated the Ca^{2+} response to orexin-A. Thus, it is possible that also other potentiators of orexin-A response may be found among the azulene derivatives presented in this study.

At that stage, the most promising compounds **11**, **17** and **28** induced an approximately two-fold increase in the Ca^{2+} response to orexin-A at 10 µM concentration. We verified the concentration-dependency of their action by testing also their potentiation effects at 1 µM and 5 µM concentrations. Limitations in water solubility of these compounds prevented us to study higher concentrations. As Figure 1E illustrates, all these compounds potentiated the effect of orexin-A in a concentration-dependent manner. Compound **28** was the best one, increasing the orexin-A response 1.4-fold at 5 µM and 2.0-fold at 10 µM concentrations. The observed potentiation by compound **28** is of similar magnitude to previously reported orexin receptor potentiators.[13] However, Lee et al. utilized a cAMP assay, and it is difficult to compare it to our results based on Ca^{2+} elevation.

Finally, we tested the effects of compounds **6**, **7**, **8**, **9**, **11**, **14**, **17**, **19**, **27**, **28**, **29** and **31** on the actions of ATP in OX_1 receptor-expressing cells. ATP causes a Ca^{2+} signal read-out similar to orexin-A, but not via the orexin receptors. None of the tested compounds affected the response to ATP in an assay set-up identical to the one used with orexin-A (Figure 1E; for all tested compounds, see Supporting Information Figure S7). Together with the absence of potentiation at the OX_2, this provides a strong evidence for a mechanism of the Ca^{2+} response potentiation to be mediated through OX_1 receptors.

Unlike the other compounds increasing the $[^{125}I]$-orexin-A binding at 10 µM concentration, compound **19** neither acted as a weak orexin receptor activator nor a potentiator of orexin-A-mediated Ca^{2+} elevation (Figure 1D). We conducted further investigations with this compound and determined K_i values of 7.5 µM and 4.9 µM for OX_1 and OX_2 receptors, respectively (Table 1; Supporting Information Figure S4).

The set of azulene compounds is congeneric, which makes it possible to draw preliminary inferences of their structure-activity relationships (SARs). For potentiation, ester in the 6-position of azulene is preferred over the corresponding carboxyl group (e.g. compounds **11** vs. **14**, and **28** vs. **29**); in contrast, for binding there is a slight preference for carboxyl group over the corresponding ester (e.g. compounds **20** vs. **21**, and **23** vs. **24**). It can be that the carboxyl group in the 6-position increases binding of the compounds to the orthosteric orexin-A binding site, or that the ester derivatives potentiate the [^{125}I]-orexin-A binding, which masks the competition between the compound and [^{125}I]-orexin-A. In the latter case, it is possible that the compounds with the ester in the 6-position actually bind better to OX$_1$ receptors than the binding data suggest. Either way, these results offer an interesting starting point for further compound development.

A consideration in this study is that we cannot critically assess the usefulness of the virtual screen. The final hit rate is high – higher that in our previously study [35] —which by itself suggests a positive influence. Nonetheless, we neither can claim for certainty that the binding site would be common among the presented azulenes, nor that it would be orthosteric. We are currently setting up assays to get an experimental answer to these questions, yet it is beyond the scope of this manuscript. Since the virtual screen was targeted at the orthosteric site, it leaves open whether we are right for the right reasons, which is a prevalent question in virtual screens. Consequently, we have avoided presenting a speculative retrospective analysis of the binding modes that would divert this manuscript from its main message. Secondly, we lack true benchmarks to assess the performance of the screen, since we do not know what would have happened without a computational selection. The compounds are congeneric, and as such expected to share some similarities in their activities, and this makes it difficult to reasonably set a "random" rate for screening. Nonetheless, this does not diminish the value of the computational selection.

3 CONCLUSIONS

Twelve novel azulene-based compounds out of 33 (four of them tested as mixtures), prioritized through a virtual screening protocol, showed noticeable binding to the orexin receptors. The two most promising binders, **22** and **32**, were orthogonally tested in a functional assay and found to have K_i values in the low micromolar range. Additionally, compounds **7** and **27** acted as weak orexin receptor agonists, inducing orexin receptor-mediated Ca^{2+} responses of 5% of the maximal response to orexin-A. This high hit rate supports the use of the prospective virtual screen, even if the protocol does not enable a fair comparison with a random selection.

A set of six compounds enhanced [^{125}I]-orexin-A binding. Upon examination of a larger compound subset, six out of twelve compounds tested showed significant potentiation of the response at sub-EC$_{50}$ concentrations of orexin-A; three of them, **11**, **17** and **28**, increased the orexin-A-mediated Ca^{2+} response in concentration-dependent manner, with two-fold potentiation at 10 μM. Previously, only one series of compounds have been reported to potentiate the actions of orexin-A.

In this study, we have presented a body of evidence that indicates a direct mechanism of action through orexin receptors: (1) weak agonism that can be suppressed by specific antagonists and evidenced in the control cells not expressing orexin receptors, (2) competition binding with [125I]-orexin-A as well as potentiation that is possibly mediated through receptor dimers, (3) potentiation of orexin-A response in OX_1 but not OX_2-expressing cells, which was significantly better than ATP controls, and (4) absence of colloidal aggregation for compounds **19**, **22** and **32** at the used concentration range. We believe that such a concordant picture point to a specific direct interaction between azulene-based compounds and orexin receptors.

How these findings translate into one or several interaction sites remains highly speculative and is beyond the scope of this manuscript. Indeed, while this study includes a significant characterization of the most intriguing compounds, the pharmacological work will extend beyond it; further studies to understand e.g. the potentiation effect and receptor dimerization need to be conducted. Furthermore, we plan to explore further the landscape of azulene derivatives to analyze their SARs. Finally, future efforts will be directed to the identification of more potent compounds.

4 EXPERIMENTAL SECTION

4.1 Computational studies. *Building the azulene-based virtual library.* An azulene scaffold was attached with three sets of manually designed R-groups (positions 1, 3 and 6; see Table 1) by combinatorial database building tool of Schrödinger Maestro 2015v1,[36] producing a database of 168084 compounds (after removing the duplicates due to the scaffold symmetry). We filtered out compounds with molecular weight over 500 g/mol, resulting in a final library of 70038 compounds. Subsequently, a set of starting points (main species predicted at pH 7 $\pm$ 2) of each compound were built by Schrödinger's LigPrep tool utilizing Epik for generating protonation states. Taking into account the possible protonation states, the library included 144000 starting points for virtual screening.

Virtual screening. To screen the virtual library we utilized Glide of Schrödinger Maestro 2015v3[23] with SP parameters. Screening was conducted on the crystal structure of OX_2 receptor[24] in the absence of the binding site waters (for more information about selecting the screening protocol see Supporting Information page S8). To monitor the performance of the docking, the virtual library was seeded with 117 dual or OX_2R selective orexin receptor antagonists. The docking protocol was able to retrieve 25% of these known actives in the top 10% of the database, with area under the accumulation curve (ROC) being 0.75. Furthermore, **40** (suvorexant), an orexin receptor antagonist present in the crystal structure, was docked among these active compounds, and the docked conformation compared to the one co-crystallized with OX_2R. Compound **40** scored to top 1.6% of the library and its conformation was highly similar to the binding conformation of **40** in the crystal structure (pairwise heavy atom RMSD 0.54 Å). Glide's "docking score"[23] was used for all ranking.

R-group analysis and compound selection. The 5% top-scoring poses (i.e. 7200 poses) were analyzed using the R-group analysis tool of Schrödinger Canvas.[23] The gained understanding

of the most favorable R-groups supported the visual examination of the 200 top-scoring docking poses.

4.2 Chemistry. All compounds were characterized by ^{1}H and ^{13}C NMR spectroscopy using a Bruker Avance III 400 MHz spectrometer. Chemical shifts are reported in parts per million (ppm) relative to the residual solvent signals: CDCl$_3$ 7.26 and 77.17 ppm, DMSO-d_6 2.50 and 39.52 ppm, acetone-d_6 2.05 and 29.84 ppm for ^{1}H and ^{13}C NMR, respectively. The progress of the reactions was monitored by thin-layer chromatography on silica gel 60-F$_{254}$ plates. Silica gel (SiO$_2$) 60 (230−400 mesh) was used in flash chromatography purifications. Microwave reactions were conducted in sealed reaction vessels using a Biotage Initiator$^+$ instrument equipped with an external IR sensor to detect the reaction temperature. Mass spectrometric analysis were performed with a Waters Synapt G2 HDMS mass spectrometer using electrospray ionization (ESI). The purity was determined by UPLC-MS with diode-array detector. The purity of the all biologically tested compounds was 95% or higher, except for **27** with 94% purity. ^{1}H NMR of **27** shows only hardly visible impurities.

6-Carboxyazulene (3). Oxone (1.23 g, 4.00 mmol) was added to a solution of 6-formylazulene (0.625 g, 4.00 mmol) in DMF (20 mL). The blue reaction mixture was stirred at room temperature for 3 h. The reaction mixture was quenched by a 1 M aqueous solution of HCl (20 mL) on ice bath and EtOAc (80 mL) was added. The organic phase was washed with a 1 M aqueous solution of HCl (3 × 60 mL) and brine (60 mL), dried over anhydrous Na$_2$SO$_4$, filtered and evaporated to provide dark green solid. The crude product was purified by flash chromatography (*n*-heptane/EtOAc/AcOH 75:24:1) to give **3** as a green, amorphous solid (0.332 g, 48%). ^{1}H NMR (400 MHz, acetone-d_6) δ 8.55 (d, *J* = 10.4 Hz, 2H), 8.11 (d, *J* = 10.8 Hz, 2H), 8.06 (t, *J* = 3.8 Hz, 1H), 7.51 (d, *J* = 3.6 Hz, 2H). ^{13}C NMR (101 MHz, acetone-d_6) δ 169.4, 142.3, 140.9, 137.4, 135.8, 123.9, 119.8. HRMS (ESI-QTOF) *m/z*: [M - H]$^-$ Calcd for C$_{11}$H$_7$O$_2$ 171.0446; Found 171.0444.

Methyl azulene-6-carboxylate (4). K$_2$CO$_3$ (0.66 g, 4.8 mmol) and iodomethane (0.24 mL, 3.8 mmol) were added to the blue solution of **3** (0.33 g, 1.9 mmol) in DMF (10 mL). The reaction mixture was stirred at room temperature for 45 min. Et$_2$O (60 mL) and a 1 M aqueous solution of HCl (30 mL) were added to the reaction mixture on ice bath. Et$_2$O phase was washed with a 1 M aqueous solution of HCl (30 mL), a saturated solution of NaHCO$_3$ (30 mL) and brine (30 mL), dried over anhydrous Na$_2$SO$_4$, filtered and evaporated to provide green-blue solid. The crude product was purified by flash chromatography (*n*-heptane/EtOAc 85:15) to give **4** as a green-blue, amorphous solid (0.34 g, 96%). ^{1}H NMR (400 MHz, CDCl$_3$) δ 8.42 (d, *J* = 10.8 Hz, 2H), 8.07–8.04 (m, 3H), 7.47 (d, *J* = 3.6 Hz, 2H), 4.00 (s, 3H). ^{13}C NMR (101 MHz, CDCl$_3$) δ 168.9, 141.5, 140.4, 136.1, 134.9, 123.2, 119.0, 53.2. HRMS (ESI-QTOF) *m/z*: [M + H]$^+$ Calcd for C$_{12}$H$_{11}$O$_2$ 187.0759; Found 187.0758.

***N,N*-Dimethyl-4-(trifluoromethyl)benzamide (5).** A 2 M solution of Me$_2$NH in THF (12.5 mL, 25.0 mmol) was added dropwise to a solution of 4-(trifluoromethyl)benzoyl chloride (1.49 mL, 10.0 mmol) in anhydrous DCM (10 mL) on ice bath under argon. The resulting mixture was stirred at 0 °C for 45 min. The reaction mixture was quenched with a 1 M aqueous solution of HCl (20 mL) on ice bath and DCM (50 mL) was added. The organic phase was washed with

a 1 M aqueous solution of HCl (2 × 30 mL), a saturated aqueous solution of NaHCO$_3$ (30 mL) and brine (30 mL), dried over anhydrous Na$_2$SO$_4$, filtered and evaporated to give **5** as a white, amorphous solid (2.17 g, quant.). ^{1}H NMR (400 MHz, CDCl$_3$) δ 7.67 (d, J = 8.0 Hz, 2H), 7.52 (d, J = 7.6 Hz, 2H), 3.12 (s, 3H), 2.96 (s, 3H). ^{13}C NMR (101 MHz, CDCl$_3$) δ 170.3, 140.0, 131.6 (q, $^2J_{C,F}$ = 32.8 Hz), 127.5, 125.6 (q, $^3J_{C,F}$ = 3.8 Hz), 123.9 (q, $^1J_{C,F}$ = 273.4 Hz), 39.5, 35.5.

General procedure for the synthesis of compounds 6, 7, 27, 28. POCl$_3$ (4 equiv) was added to a solution of the appropriate azulene derivative and *N,N*-dimethylbenzamide derivative (4.3 equiv) in anhydrous 1,4-dioxane (4 mL) under argon. The resulting solution was heated under microwave irradiation at 100 °C for 2–5 h. The reaction mixture was poured into a 1 M aqueous solution of NaOH (80–100 mL) and extracted with DCM (60 + 30 mL). The organic phases were combined and washed with water (50 mL), dried over anhydrous Na$_2$SO$_4$, filtered and evaporated to provide a crude product, which was purified by flash chromatography.

Methyl 1-benzoylazulene-6-carboxylate (6). Compound **4** (0.317 g, 1.70 mmol) and *N,N*-dimethylbenzamide (1.09 g, 7.30 mmol) with a 3-h reaction time gave a green-blue oil, which after flash chromatography (*n*-heptane/EtOAc 85:15) yielded **6** as a green, amorphous solid (0.309 g, 63%). ^{1}H NMR (400 MHz, CDCl$_3$) δ 9.73 (d, J = 10.4 Hz, 1H), 8.57 (d, J = 10.4 Hz, 1H), 8.46 (dd, J = 10.4, 1.6 Hz, 1H), 8.32 (dd, J = 10.4, 1.6 Hz, 1H), 8.22 (d, J = 4.4 Hz, 1H), 7.87–7.84 (m, 2H), 7.60–7.56 (m, 1H), 7.53–7.49 (m, 2H), 7.37 (d, J = 4.4 Hz, 1H), 4.04 (s, 3H). ^{13}C NMR (101 MHz, CDCl$_3$) δ 192.9, 168.0, 146.0, 145.2, 142.8, 141.0, 138.2, 137.6, 137.1, 131.6, 129.7, 129.2, 128.4, 127.4, 125.9, 118.6, 53.5. HRMS (ESI-QTOF) *m/z*: [M + H]$^+$ Calcd for C$_{19}$H$_{15}$O$_3$ 291.1021; Found 291.1025.

Methyl 1-[4-(trifluoromethyl)benzoyl]azulene-6-carboxylate (7). Compound **4** (0.372 g, 2.00 mmol) and **5** (1.09 g, 7.30 mmol) with a 5-h reaction time gave a green solid, which after flash chromatography (*n*-heptane/EtOAc 85:15) yielded **7** as a green, amorphous solid (0.540 g, 75%). ^{1}H NMR (400 MHz, CDCl$_3$) δ 9.80 (d, J = 10.4 Hz, 1H), 8.60 (d, J = 10.4 Hz, 1H), 8.51 (dd, J = 10.4, 1.6 Hz, 1H), 8.37 (dd, J = 10.4, 1.6 Hz, 1H), 8.14 (d, J = 4.4 Hz, 1H), 7.93 (d, J = 8.0 Hz, 2H), 7.78 (d, J = 8.0 Hz, 2H), 7.37 (d, J = 4.4 Hz, 1H), 4.05 (s, 3H). ^{13}C NMR (101 MHz, CDCl$_3$) δ 191.5, 167.8, 146.5, 145.1, 144.2, 143.1, 138.6, 137.9, 137.4, 133.0 (q, $^2J_{C,F}$ = 32.7 Hz), 129.8, 129.7, 128.0, 125.4 (q, $^3J_{C,F}$ = 3.8 Hz), 125.1, 122.6, 118.9, 53.6. HRMS (ESI-QTOF) *m/z*: [M + H]$^+$ Calcd for C$_{20}$H$_{14}$O$_3$F$_3$ 359.0895; Found 359.0897.

Methyl 2-(1-benzoylazulen-6-yl)acetate (27). Compound **26** (0.521 g, 2.60 mmol) and *N,N*-dimethylbenzamide (1.68 g, 11.2 mmol) with a 2-h reaction time gave a brown oil, which after flash chromatography (*n*-heptane/EtOAc 3:1) yielded **27** as a purple, amorphous solid (0.310 g, 39%). ^{1}H NMR (400 MHz, CDCl$_3$) δ 9.63 (d, J = 10.0 Hz, 1H), 8.44 (d, J = 10.0 Hz, 1H), 8.05 (d, J = 4.0 Hz, 1H), 7.85–7.83 (m, 2H), 7.59–7.54 (m, 2H), 7.52–7.46 (m, 3H), 7.28 (d, J = 4.4 Hz, 1H), 3.91 (s, 2H), 3.73 (s, 3H). ^{13}C NMR (101 MHz, CDCl$_3$) δ 193.0, 171.1, 146.4, 144.4, 142.5, 141.4, 140.8, 138.5, 137.8, 131.3, 130.7, 129.7, 129.2, 128.2, 125.6, 118.2, 52.6, 46.8. HRMS (ESI-QTOF) *m/z*: [M + H]$^+$ Calcd for C$_{20}$H$_{17}$O$_3$ 305.1178; Found 305.1176.

Methyl 2-[1-[4-(trifluoromethyl)benzoyl]azulen-6-yl]acetate (28). Compound **26** (0.400 g, 2.00 mmol) and **5** (1.87 g, 8.60 mmol) with a 2-h reaction time gave a brown solid, which after flash chromatography (manual gradient of *n*-heptane/EtOAc 3:1 → 2:1) yielded **28** as a

purple, amorphous solid (0.322 g, 43%). ^{1}H NMR (400 MHz, CDCl$_3$) δ 9.69 (d, J = 10.0 Hz, 1H), 8.46 (d, J 10.0 Hz, 1H), 7.97 (d, J = 4.0 Hz, 1H), 7.92 (d, J = 8.0 Hz, 2H), 7.76 (d, J = 8.0 Hz, 2H), 7.63 (dd, J = 10.2, 1.8 Hz, 1H), 7.52 (dd, J = 10.4, 1.6 Hz, 1H), 7.28 (d, J = 4.4 Hz, 1H), 3.93 (s, 2H), 3.73 (s, 3H). ^{13}C NMR (101 MHz, CDCl$_3$) δ 191.5, 171.0, 146.9, 144.8, 144.6, 142.4, 141.0, 138.7, 138.1, 132.7 (q, $^2J_{C,F}$ = 32.6 Hz), 131.4, 129.9, 129.7, 125.3 (q, $^3J_{C,F}$ = 3.8 Hz), 124.7, 124.0 (q, $^1J_{C,F}$ = 273.5 Hz), 118.5, 52.6, 46.8. HRMS (ESI-QTOF) m/z: [M + H]$^+$ Calcd for C$_{21}$H$_{16}$O$_3$F$_3$ 373.1052; Found 373.1052.

General procedure for the synthesis of compounds 8, 9, 14, 19. The appropriate ester derivative was dissolved in THF (2–13 mL) and MeOH (0.2–0.65 mL). A 2 M aqueous solution of NaOH (0.2–2.2 mL) was added to the blue solution and the resulting mixture was stirred at room temperature for 1–28 h. A 1 M aqueous solution of HCl (5 mL) was added to the reaction mixture on ice bath and then the mixture was extracted with EtOAc (40–50 mL). The organic phase was washed with a 1 M aqueous solution of HCl (2 × 20–25 mL) and brine (20–25 mL), dried over anhydrous Na$_2$SO$_4$, filtered and evaporated to provide a crude product, which was purified by flash chromatography.

1-Benzoylazulene-6-carboxylic acid (8). Compound **6** (0.099 g, 0.34 mmol) with a 1.5-h reaction time gave a green solid, which after flash chromatography (EtOAc/AcOH 99:1) yielded **8** as a green, amorphous solid (0.077 g, 82%). ^{1}H NMR (400 MHz, DMSO-d_6) δ 9.62 (d, J = 10.4 Hz, 1H), 8.81 (d, J = 10.4 Hz, 1H), 8.44 (dd, J = 10.4, 1.6 Hz, 1H), 8.33 (dd, J = 10.0, 1.6 Hz, 1H), 8.18 (d, J = 4.4 Hz, 1H), 7.80–7.77 (m, 2H), 7.67–7.62 (m, 1H), 7.59–7.54 (m, 2H), 7.51 (d, J = 4.4 Hz, 1H). ^{13}C NMR (101 MHz, DMSO-d_6) δ 191.5, 168.3, 145.3, 144.3, 141.7, 140.4, 139.6, 137.9, 137.0, 131.6, 129.1, 128.8, 128.4, 127.6, 124.7, 118.8. HRMS (ESI-QTOF) m/z: [M + H]$^+$ Calcd for C$_{18}$H$_{13}$O$_3$ 277.0865; Found 277.0866

1-[4-(Trifluoromethyl)benzoyl]azulene-6-carboxylic acid (9). Compound **7** (0.047 g, 0.13 mmol) with a 1.5-h reaction time gave a green-blue solid, which after flash chromatography (EtOAc/AcOH 99:1) yielded **9** as a dark green, amorphous solid (0.039 g, 87%). ^{1}H NMR (400 MHz, DMSO-d_6) δ 9.70 (d, J = 10.4 Hz, 1H), 8.85 (d, J = 10.4 Hz, 1H), 8.50 (dd, J = 10.4, 1.6 Hz, 1H), 8.38 (dd, J = 10.2, 1.4 Hz, 1H), 8.17 (d, J = 4.4 Hz, 1H), 7.98–7.92 (m, 4H), 7.52 (d, J = 4.0 Hz, 1H). ^{13}C NMR (101 MHz, DMSO-d_6) δ 190.3, 168.2, 145.8, 144.6, 144.1, 142.0, 140.2, 138.2, 137.3, 131.0 (q, $^2J_{C,F}$ = 31.9 Hz), 129.7, 129.6, 128.2, 125.4 (q, $^3J_{C,F}$ = 3.8 Hz), 124.0 (q, $^1J_{C,F}$ = 273.5 Hz), 123.9, 119.1. HRMS (ESI-QTOF) m/z: [M + H]$^+$ Calcd for C$_{19}$H$_{12}$O$_3$F$_3$ 345.0739; Found 345.0741.

1,3-Dibenzoylazulene-6-carboxylic acid (14). Compound **11** (0.12 g, 0.30 mmol) with a 1-h reaction time gave a brown solid, which after flash chromatography (manual gradient of THF/AcOH/MeOH 99:1:1 → 96:2:2) yielded **14** as a green, amorphous solid (0.039 g, 34%). ^{1}H NMR (400 MHz, DMSO-d_6) δ 9.83 (d, J = 11.2 Hz, 2H), 8.75 (d, J = 11.2 Hz, 2H), 8.17 (s, 1H), 7.85–7.82 (m, 4H), 7.65–7.61 (m, 2H), 7.57–7.53 (m, 4H). ^{13}C NMR (101 MHz, DMSO-d_6) δ 191.6, 167.9, 147.9, 144.8, 143.6, 139.8, 139.1, 132.6, 132.0, 129.3, 128.5, 123.4. HRMS (ESI-QTOF) m/z: [M + H]$^+$ Calcd for C$_{25}$H$_{17}$O$_4$ 381.1127; Found 381.1128

1-Benzoyl-3-(4-ethoxyphenyl)azulene-6-carboxylic acid (19). Compound **18** (0.17 g, 0.42 mmol) with a 28-h reaction time gave a brown solid, which after flash chromatography (EtOAc/AcOH 99:1) yielded a brownish green solid. The solid was washed an equimixture of

DCM and EtOAc to give **19** as a brownish green, amorphous solid (0.010 g, 6%). ^{1}H NMR (400 MHz, DMSO-d_6) δ 9.59 (d, J = 10.4 Hz, 1H), 8.78 (d, J = 10.4 Hz, 1H), 8.38 (d, J = 10.4 Hz, 1H), 8.28 (d, J = 10.4 Hz, 1H), 8.19 (s, 1H), 7.85–7.83 (m, 2H), 7.66–7.63 (m, 1H), 7.58–7.55 (m, 4H), 7.08–7.06 (m, 2H), 4.09 (q, J = 7.0 Hz, 2H), 1.36 (t, J = 7.0 Hz, 3H). ^{13}C NMR (101 MHz, DMSO-d_6) δ 191.4, 168.2, 157.9, 143.5, 142.5, 140.5, 140.3, 139.7, 137.3, 136.3, 131.7, 130.7, 130.5, 129.3, 128.8, 128.5, 127.7, 127.3, 123.6, 114.9, 63.2, 14.7. HRMS (ESI-QTOF) *m/z*: [M + H]$^+$ Calcd for $C_{26}H_{21}O_4$ 397.1440; Found 397.1440.

1-Benzoylazulene-6-carboxamide (10). Compound **8** (0.069 g, 0.25 mmol) was dissolved in DMF (1 mL). The blue solution was cooled to 0 °C and EDC·HCl (0.053 g, 0.28 mmol) and HOBt·H$_2$O (0.043 g, 0.28 mmol) were added. The reaction mixture was stirred at 0 °C for 15 min and at room temperature for 1 h. Aqueous NH$_3$ (25%, 0.048 mL, 0.63 mmol) was added and the stirring was continued at room temperature for 2.5 h. H$_2$O (15 mL) was added to the reaction mixture and it was extracted with EtOAc (30 mL). The organic phase was washed with a 1 M aqueous solution of HCl (15 mL) and a saturated aqueous solution of NaHCO$_3$ (15 mL), dried over anhydrous Na$_2$SO$_4$, filtered and evaporated to provide a green solid. The crude product was purified by flash chromatography (EtOAc/MeOH/Et$_3$N 93:5:2) to give **10** as a green, amorphous solid (0.060 g, 87%). ^{1}H NMR (400 MHz, DMSO-d_6) δ 9.59 (d, J = 10.4 Hz, 1H), 8.79 (d, J = 10.4 Hz, 1H), 8.35 (s, 1H), 8.13–8.10 (m, 2H), 8.03 (dd, J = 10.2, 1.4 Hz, 1H), 7.81 (s, 1H), 7.79–7.77 (m, 2H), 7.66–7.62 (m, 1H), 7.59–7.55 (m, 2H), 7.49 (d, J = 4.0 Hz, 1H). ^{13}C NMR (101 MHz, DMSO-d_6) δ 191.5, 170.1, 145.1, 144.8, 143.4, 141.0, 140.5, 138.4, 137.4, 131.5, 129.1, 128.4, 127.5, 126.6, 124.5, 118.5. HRMS (ESI-QTOF) m/z: [M + H]$^+$ Calcd for $C_{18}H_{14}NO_2$ 276.1024; Found 276.1026.

Methyl 1,3-dibenzoylazulene-6-carboxylate (11). Compound **6** (0.15 g, 0.50 mmol) and benzoyl chloride (0.087 mL, 0.75 mmol) were dissolved in anhydrous DCM (3 mL) under argon. The reaction mixture was cooled to 0 °C and AlCl$_3$ (0.13 g, 1.0 mmol) was added. The brownish red solution was stirred at 0 °C for 30 min and at room temperature for 4 h. An additional 1 equiv of AlCl$_3$ (0.067 g, 0.50 mmol) and 1.5 equiv of benzoyl chloride (0.087 mL, 0.75 mmol) were added, and stirring was continued at room temperature for 20 h. The reaction mixture was quenched by a 1 M aqueous solution of HCl (5 mL) on ice bath and DCM (50 mL) was added. Phases were separated and the organic phase was washed with a 1 M aqueous solution of HCl (2 × 25 mL), a saturated solution of NaHCO$_3$ (25 mL) and water (25 mL), dried over anhydrous Na$_2$SO$_4$, filtered and evaporated to provide greenish brown solid. The crude product was purified by flash chromatography (*n*-heptane/DCM 1:3 + *n*-heptane/DCM/EtOAc 25:70:5) to give **11** as a dark gray, amorphous solid (0.17 g, 87%). ^{1}H NMR (400 MHz, CDCl$_3$) δ 9.85 (d, J = 10.8 Hz, 2H), 8.67 (d, J = 11.2 Hz, 2H), 8.36 (s, 1H), 7.86–7.83 (m, 4H), 7.59–7.55 (m, 2H), 7.51–7.47 (m, 4H), 4.08 (s, 3H). ^{13}C NMR (101 MHz, CDCl$_3$) δ 192.8, 167.3, 148.6, 145.9, 140.3, 140.2, 139.3, 132.2, 132.0, 129.8, 128.5, 124.9, 53.8. HRMS (ESI-QTOF) *m/z*: [M + H]$^+$ Calcd for $C_{26}H_{19}O_4$ 395.1283; Found 395.1288.

Methyl 1-benzoyl-3-iodoazulene-6-carboxylate (17). Compound **6** (0.058 g, 0.20 mmol) was dissolved in anhydrous DCM (1 mL) under argon. The blue solution was cooled to 0 °C and NIS (0.11 g, 0.50 mmol) was added. The mixture was stirred at 0 °C for 1 h and then at room temperature for 3.5 h. The reaction mixture was eluted through a pad of neutral alumina

with DCM (10 mL) and concentrated *in vacuo* to give **17** as a green, amorphous solid (0.081 g, 98%). ^{1}H NMR (400 MHz, acetone-d_6) δ 9.63 (d, J = 10.4 Hz, 1H), 8.63 (d, J = 10.8 Hz, 1H), 8.53–8.48 (m, 2H), 8.33 (s, 1H), 7.87–7.85 (m, 2H), 7.69–7.64 (m, 1H), 7.61–7.57 (m, 2H), 4.04 (s, 3H). ^{13}C NMR (101 MHz, acetone-d_6) δ 191.6, 167.9, 151.6, 145.3, 143.1, 141.3, 140.3, 137.9, 132.6, 130.4, 130.2, 129.3, 128.7, 127.9, 77.0, 53.9. HRMS (ESI-QTOF) *m/z*: [M + H]$^+$ Calcd for $C_{19}H_{14}O_3I$ 416.9987; Found 416.9988.

Methyl 1-benzoyl-3-(4-ethoxyphenyl)azulene-6-carboxylate (18). A mixture of compound **17** (0.071 g, 0.17 mmol), 4-ethoxyphenylboronic acid (0.056 g, 0.34 mmol), Pd(dppf)Cl$_2$ (0.0062 g, 0.0085 mmol), BINAP (0.0053 g, 0.0085 mmol) and Cs$_2$CO$_3$ (0.22 g, 0.68 mmol) in anhydrous toluene (2.5 mL) was heated under microwave irradiation 110 °C for 1 h under argon. The resulting green mixture was filtered through a small pad of Celite with DCM (5 mL) and diluted with DCM (20 mL). The organic phase was washed with water (15 mL), a saturated aqueous solution of NaHCO$_3$ (15 mL) and brine (15 mL), dried over anhydrous Na$_2$SO$_4$, filtered and evaporated to provide a dark green oil. The crude product was purified by flash chromatography (manual gradient of *n*-heptane/DCM/EtOAc 1:1:0 → 47.5:47.5:5) to give **18** as a green, amorphous solid (0.059, 84%). ^{1}H NMR (400 MHz, CDCl$_3$) δ 9.70 (d, J = 10.0 Hz, 1H), 8.70 (d, J = 10.4 Hz, 1H), 8.39 (dd, J = 10.4, 1.6 Hz, 1H), 8.25 (s, 1H), 8.23 (dd, J = 10.4, 1.6 Hz, 1H), 7.89–7.87 (m, 2H), 7.60–7.56 (m, 1H), 7.53–7.46 (m, 4H), 7.06–7.02 (m, 2H), 4.12 (q, J = 7.0 Hz, 2H), 4.03 (s, 3H), 1.47 (t, J = 7.0 Hz, 3H). ^{13}C NMR (101 MHz, CDCl$_3$) δ 192.8, 168.0, 158.6, 144.8, 143.6, 141.0, 138.7, 137.8, 135.9, 131.7, 131.7, 130.9, 129.8, 129.0, 128.4, 128.0, 127.2, 124.7, 115.1, 63.8, 53.5, 15.0. HRMS (ESI-QTOF) *m/z*: [M + H]$^+$ Calcd for $C_{27}H_{23}O_4$ 411.1596; Found 411.1596.

Methyl 1-formylazulene-6-carboxylate (20). Compound **4** (0.384 g, 2.06 mmol) was dissolved in anhydrous DCM (10 mL) under argon. (Chloromethylene)dimethyliminium chloride (0.291 g, 2.27 mmol) in anhydrous DCM (15 mL) was added to the blue solution at 0 °C. The resulting mixture was stirred at 0 °C for 60 min. A 1 M aqueous solution of NaOH (80 mL) and DCM (25 mL) were added to the reaction mixture on ice bath. Phases were separated and aqueous phase was extracted with DCM (30 mL). DCM phases were combined and washed with water (50 mL), dried over anhydrous Na$_2$SO$_4$, filtered and evaporated to provide a dark green solid. The crude product was purified by flash chromatography (*n*-heptane/EtOAc 2:1) to give **20** as a green, amorphous solid (0.271 g, 61%). ^{1}H NMR (400 MHz, acetone-d_6) δ 10.44 (s, 1H), 9.61 (d, J = 10.4 Hz, 1H), 8.77 (d, J = 10.4 Hz, 1H), 8.49 (d, J = 4.0 Hz, 1H), 8.44 (dd, J = 10.2, 1.4 Hz, 1H), 8.34 (dd, J = 10.4, 1.6 Hz, 1H), 7.54 (d, J = 4.0 Hz, 1H), 4.02 (s, 3H). ^{13}C NMR (101 MHz, acetone-d_6) δ 186.8, 168.1, 147.4, 144.9, 141.8, 139.5, 138.8, 136.3, 129.7, 128.6, 127.8, 120.9, 53.7. HRMS (ESI-QTOF) *m/z*: [M + H]$^+$ Calcd for $C_{13}H_{11}O_3$ 215.0708; Found 215.0708.

1-Formylazulene-6-carboxylic acid (21). The purple NaOH phase from the reaction of **20** was acidified with a 37% solution of HCl in H$_2$O, and it was extracted with EtOAc (80 mL). The organic phase was washed with brine (40 mL), dried over anhydrous Na$_2$SO$_4$, filtered and evaporated to give **21** as a brownish green, amorphous solid (0.061 g, 15%). ^{1}H NMR (400 MHz, DMSO-d_6) δ 10.40 (s, 1H), 9.56 (d, J = 10.4 Hz, 1H), 8.82 (d, J = 10.0 Hz, 1H), 8.50 (d, J = 4.0 Hz, 1H), 8.44 (dd, J = 10.4, 1.6 Hz, 1H), 8.35 (dd, J = 10.2, 1.4 Hz, 1H), 7.57 (d, J =

4.4 Hz, 1H). ^{13}C NMR (101 MHz, DMSO-d_6) δ 186.4, 168.2, 146.1, 143.3, 140.9, 139.7, 138.4, 135.3, 129.1, 128.3, 126.2, 120.1. HRMS (ESI-QTOF) m/z: [M + H]$^+$ Calcd for C$_{12}$H$_9$O$_3$ 201.0552; Found 201.0556.

Methyl 1-formyl-3-iodoazulene-6-carboxylate (22). Compound **20** (0.257 g, 1.20 mmol) was dissolved in anhydrous DCM (3 mL) under argon. The blue solution was cooled to 0 °C and NIS (0.270 g, 1.20 mmol) was added. The mixture was stirred at 0 °C for 30 min, an additional 1.5 equiv of NIS (0.405 g, 1.80 mmol) was added, and stirring was continued at 0 °C for 1 h and then at room temperature for 19 h. The reaction mixture was eluted through a pad of neutral alumina with DCM and concentrated *in vacuo* to give **22** as a green, amorphous solid (0.401 g, 98%). ^{1}H NMR (400 MHz, acetone-d_6) δ 10.38 (s, 1H), 9.60 (d, J = 10.4 Hz, 1H), 8.63 (s, 1H), 8.61 (d, J = 10.4 Hz, 1H), 8.53–8.49 (m, 2H), 4.04 (s, 3H). ^{13}C NMR (101 MHz, acetone-d_6) δ 186.1, 167.8, 151.7, 146.1, 141.8, 140.7, 140.4, 136.4, 130.9, 129.4, 128.9, 78.2, 53.9. HRMS (ESI-QTOF) m/z: [M + H]$^+$ Calcd for C$_{13}$H$_{10}$O$_3$I 340.9675; Found 340.9673.

Methyl 1-formyl-3-phenylazulene-6-carboxylate (23). A mixture of compound **22** (0.34 g, 1.0 mmol), phenylboronic acid (0.24 g, 2.0 mmol), Pd(dppf)Cl$_2$ (0.037 g, 0.050 mmol), BINAP (0.031 g, 0.050 mmol) and Cs$_2$CO$_3$ (1.3 g, 4.0 mmol) in anhydrous toluene (15 mL) was heated under microwave irradiation 110 °C for 1 h under argon. The resulting brownish green mixture was filtered through a small pad of Celite with DCM (20 mL) and diluted with DCM (60 mL). The organic phase was washed with water (50 mL), a saturated aqueous solution of NaHCO$_3$ (50 mL) and brine (50 mL), dried over anhydrous Na$_2$SO$_4$, filtered and evaporated to provide a green solid. The crude product was purified by flash chromatography (DCM) to give **23** as a green, amorphous solid (0.25 g, 88%). ^{1}H NMR (400 MHz, CDCl$_3$) δ 10.46 (s, 1H), 9.65 (d, J = 10.0 Hz, 1H), 8.74 (d, J = 10.4 Hz, 1H), 8.49 (s, 1H), 8.43 (dd, J = 10.2, 1.4 Hz, 1H), 8.30 (dd, J = 10.4, 1.6 Hz, 1H), 7.60–7.52 (m, 4H), 7.46–7.42 (m, 1H), 4.04 (s, 3H). ^{13}C NMR (101 MHz, CDCl$_3$) δ 186.6, 167.6, 144.4, 142.5, 142.1, 139.0, 136.4, 136.3, 135.5, 133.3, 129.7, 129.1, 128.3, 127.6, 125.5, 53.56. HRMS (ESI-QTOF) m/z: [M + H]$^+$ Calcd for C$_{19}$H$_{15}$O$_3$ 291.1021; Found 291.1026.

1-Formyl-3-phenylazulene-6-carboxylic acid (24). Compound **23** (0.17 g, 0.60 mmol) was dissolved in THF (3 mL). A 2 M aqueous solution of NaOH (1.5 mL) was added to the blue solution and the resulting mixture was stirred at room temperature for 2 h. A 1 M aqueous solution of HCl (5 mL) was added to the reaction mixture on ice bath and then the mixture was extracted with EtOAc (50 mL). The organic phase was washed with a 1 M aqueous solution of HCl (2 × 25 mL) and brine (25 mL), dried over anhydrous Na$_2$SO$_4$, filtered and evaporated. The residue was washed with DCM (20 mL) and water (20 mL) and then the blue solid was dissolved in THF. THF was evaporated to give **24** as a green-blue, amorphous solid (0.15 g, 92%). ^{1}H NMR (400 MHz, DMSO-d_6) δ 10.44 (s, 1H), 9.59 (d, J = 10.4 Hz, 1H), 8.82 (d, J = 10.4 Hz, 1H), 8.61 (s, 1H), 8.40 (dd, J = 10.2, 1.4 Hz, 1H), 8.33 (dd, J = 10.6, 1.4 Hz, 1H), 7.67–7.54 (m, 2H), 7.58–7.54 (m, 2H), 7.46–7.42 (m, 1H). ^{13}C NMR (101 MHz, DMSO-d_6) δ 186.5, 168.0, 143.1, 141.8, 140.9, 140.3, 136.8, 135.8, 135.0, 132.1, 129.4, 129.3, 129.0, 128.7, 127.3, 125.0. HRMS (ESI-QTOF) m/z: [M + H]$^+$ Calcd for C$_{18}$H$_{13}$O$_3$ 277.0865; Found 277.0870.

1-Formyl-3-phenylazulene-6-carboxamide (25). Compound **24** (0.055 g, 0.20 mmol) was dissolved in DMF (1 mL). The blue solution was cooled to 0 °C and EDC·HCl (0.042 g, 0.22 mmol) and HOBt·H$_2$O (0.034 g, 0.22 mmol) were added. The reaction mixture was stirred at 0 °C for 15 min and at room temperature for 1 h. Aqueous NH$_3$ (25%, 0.037 mL, 0.50 mmol) was added and the stirring was continued at room temperature for 3.5 h. H$_2$O (15 mL) was added to the reaction mixture and it was extracted with EtOAc (30 mL). The organic phase was washed with a 1 M aqueous solution of HCl (15 mL) and a saturated aqueous solution of NaHCO$_3$ (15 mL), dried over anhydrous Na$_2$SO$_4$, filtered and evaporated to provide a blue solid. The crude product was purified by flash chromatography (manual gradient of EtOAc/MeOH 1:0 → 3:1) to give **25** as a green, amorphous solid (0.019 g, 35%). ^{1}H NMR (400 MHz, DMSO-d_6) δ 10.45 (s, 1H), 9.58 (d, J = 10.0 Hz, 1H), 8.79 (d, J = 10.4 Hz, 1H), 8.57 (s, 1H), 8.35 (s, 1H), 8.09 (dd, J = 10.2, 1.4 Hz, 1H), 8.04 (dd, J = 10.4, 1.6 Hz, 1H), 7.83 (s, 1H), 7.66 (d, J = 7.6 Hz, 2H), 7.56 (t, J = 7.6 Hz, 2H), 7.44 (t, J = 7.4 Hz, 1H). ^{13}C NMR (101 MHz, DMSO-d_6) δ 186.6, 169.9, 146.0, 142.1, 141.1, 140.3, 137.1, 136.4, 135.1, 131.9, 129.4, 129.0, 128.0, 127.7, 127.3, 124.9. HRMS (ESI-QTOF) m/z: [M + H]$^+$ Calcd for C$_{18}$H$_{14}$NO$_2$ 276.1024; Found 276.1030.

Methyl 2-(azulen-6-yl)acetate (26). 6-Methylazulene (0.71 g, 5.0 mmol) was dissolved in anhydrous THF (20 mL) under argon. A 1 M solution of LDA in hexane/THF (5.5 mL, 5.5 mmol) was added to the blue solution at 0 °C. The solution turned dark red and was first stirred at 0 °C for 10 min and then at room temperature for 20 min. The solution was cooled to −78 °C and methyl chloroformate (0.39 mL, 5.0 mmol) was added. The solution was stirred at −78 °C for 10 min and then allowed to warm to 0 °C over a period of 45 min. The mixture was quenched with a 1 M aqueous solution of HCl (10 mL) and it was extracted with EtOAc (80 mL). The organic phase was washed with a 1 M aqueous solution of HCl (2 × 40 mL), a saturated aqueous solution of NaHCO$_3$ (2 × 40 mL) and brine (40 mL), dried over anhydrous Na$_2$SO$_4$, filtered and evaporated to provide a blue oil. The crude product was purified by flash chromatography (manual gradient of n-heptane/DCM 4:1 → 0:1) to give **26** as a blue, amorphous solid (0.52 g, 52%). ^{1}H NMR (400 MHz, CDCl$_3$) δ 8.29 (d, J = 10.4 Hz, 2H), 7.89 (t, J = 3.8 Hz, 1H), 7.39 (d, J = 3.6 Hz, 2H), 7.15 (d, J = 10.4 Hz, 2H), 3.82 (s, 2H), 3.72 (s, 3H). ^{13}C NMR (101 MHz, CDCl$_3$) δ 171.7, 143.6, 139.4, 137.1, 135.8, 124.5, 118.7, 52.4, 47.0. HRMS (ESI-QTOF) m/z: [M + H]$^+$ Calcd for C$_{13}$H$_{13}$O$_2$ 201.0916; Found 201.0917.

2-[1-[4-(Trifluoromethyl)benzoyl]azulen-6-yl]acetic acid (29). Compound **28** (0.15 g, 0.40 mmol) was dissolved in THF (5 mL). A 0.1 M aqueous solution of NaOH (5 mL) was added to the red solution and the resulting mixture was stirred at room temperature for 3.5 h. A 1 M aqueous solution of HCl (5 mL) was added to the reaction mixture on ice bath and then the mixture was extracted with EtOAc (40 mL). The organic phase was washed with a 1 M aqueous solution of HCl (2 × 20 mL) and brine (20 mL), dried over anhydrous Na$_2$SO$_4$, filtered and evaporated to provide a red solid. The crude product was purified by flash chromatography (manual gradient of EtOAc/AcOH 1:0 → 99:1) to give **29** as a red, amorphous solid (0.11 g, 78%). ^{1}H NMR (400 MHz, CDCl$_3$) δ 9.69 (d, J = 10.0 Hz, 1H), 8.47 (d, J = 10.0 Hz, 1H), 7.98 (d, J = 4.4 Hz, 1H), 7.92 (d, J = 7.6 Hz, 2H), 7.76 (d, J = 8.4 Hz, 2H), 7.63 (dd, J = 9.8, 1.8, 1H), 7.52 (dd, J = 10.2, 1.8 Hz, 1H), 7.29 (d, J = 4.0 Hz, 1H), 3.96 (s, 2H). ^{13}C NMR (101

MHz, CDCl$_3$) δ 191.6, 174.8, 146.0, 144.9, 144.5, 142.6, 141.1, 138.7, 138.1, 132.8 (q, $^2J_{C,F}$ = 32.6 Hz), 131.4, 129.9, 129.7, 125.3 (q, $^3J_{C,F}$ = 3.8 Hz), 124.8, 124.0 (q, $^1J_{C,F}$ = 273.5 Hz), 118.7, 46.3. Compound **29** decarboxylated during the HRMS analysis and only **30** was detected, when **29** was ionized with ESI or APPI/APCI ion source. HRMS (ESI-QTOF) *m/z*: [M + H]$^+$ Calcd for C$_{19}$H$_{14}$OF$_3$ 315.0997; Found 315.0999.

(6-Methylazulen-1-yl)[4-(trifluoromethyl)phenyl]methanone (30). Compound **29** (0.076 g, 0.21 mmol) was dissolved in DMF (1 mL). The red solution was cooled to 0 °C and EDC·HCl (0.044 g, 0.23 mmol) and HOBt·H$_2$O (0.035 g, 0.23 mmol) were added. The reaction mixture was stirred at 0 °C for 15 min and at room temperature for 1 h. Aqueous NH$_3$ (25%, 0.040 mL, 0.53 mmol) was added and the stirring was continued at room temperature for 4 h. H$_2$O (15 mL) was added to the reaction mixture and it was extracted with EtOAc (30 mL). The organic phase was washed with a 1 M aqueous solution of HCl (15 mL) and a saturated solution of NaHCO$_3$ (15 mL), dried over anhydrous Na$_2$SO$_4$, filtered and evaporated to provide a purple solid. The crude product was purified by flash chromatography (*n*-heptane/EtOAc 1:3) to give **30** as a purple, amorphous solid (0.056 g, 85%). ^{1}H NMR (400 MHz, CDCl$_3$) δ 9.66 (d, *J* = 10.4 Hz, 1H), 8.39 (d, *J* = 10.4 Hz, 1H), 7.92 (d, *J* = 8.0 Hz, 2H), 7.89 (d, *J* = 4.4 Hz, 1H), 7.75 (d, *J* = 8.0 Hz, 2H), 7.60 (dd, *J* = 10.6, 1.4 Hz, 1H), 7.48 (dd, *J* = 10.0, 1.2 Hz, 1H), 7.22 (d, *J* = 4.0 Hz, 1H), 2.77 (s, 3H). ^{13}C NMR (101 MHz, CDCl$_3$) δ 191.5, 152.7, 144.9, 144.5, 141.3, 140.6, 138.8, 138.1, 132.5 (q, $^2J_{C,F}$ = 32.6 Hz), 131.3, 130.1, 129.7, 125.2 (q, $^3J_{C,F}$ = 3.8 Hz), 124.3, 124.1 (q, $^1J_{C,F}$ = 273.5 Hz), 118.1, 28.3. HRMS (ESI-QTOF) *m/z*: [M + H]$^+$ Calcd for C$_{19}$H$_{14}$OF$_3$ 315.0997; Found 315.1001.

Methyl 2-(1,3-dibenzoylazulen-6-yl)acetate (31). Compound **27** (0.061 g, 0.20 mmol) and benzoyl chloride (0.035 mL, 0.30 mmol) were dissolved in anhydrous DCM (1 mL) under argon. The reaction mixture was cooled to 0 °C and AlCl$_3$ (0.053 g, 0.40 mmol) was added. The orange-red solution was stirred at 0 °C for 30 min and at room temperature for 2.5 h. An additional 1 equiv of AlCl$_3$ (0.027 g, 0.20 mmol) and 1.5 equiv of benzoyl chloride (0.035 mL, 0.30 mmol) were added, and stirring was continued at room temperature for 3 h. The reaction mixture was quenched by a few drops of a 1 M aqueous solution of HCl on ice bath and DCM (25 mL) was added. The organic phase was washed with a 1 M aqueous solution of HCl (2 × 25 mL), a saturated solution of NaHCO$_3$ (25 mL) and water (25 mL), dried over anhydrous Na$_2$SO$_4$, filtered and evaporated to provide red solid. The crude product was purified by flash chromatography (manual gradient of *n*-heptane/DCM 1:1 → 0:1 + DCM/EtOAc 95:5) to give **31** as a red, amorphous solid (0.060 g, 73%). ^{1}H NMR (400 MHz, CDCl$_3$) δ 9.77 (d, *J* = 10.8 Hz, 2H), 8.21 (s, 1H), 7.85–7.82 (m, 6H), 7.57–7.53 (m, 2H), 7.50–7.45 (m, 4H), 4.01 (s, 2H), 3.75 (s, 3H). ^{13}C NMR (101 MHz, CDCl$_3$) δ 193.0, 170.5, 149.2, 146.6, 144.2, 140.5, 140.0, 134.0, 132.0, 129.7, 128.5, 124.4, 52.8, 46.7. HRMS (ESI-QTOF) *m/z*: [M + H]$^+$ Calcd for C$_{27}$H$_{21}$O$_4$ 409.1440; Found 409.1441.

4.3 Biology. *Materials.* Human orexin-A was from NeoMPS (Strasbourg, France), Dyngo 4a, i.e. 3-hydroxy-*N'*-[(2,4,5-trihydroxyphenyl)methylidene]naphthalene-2-carbohydrazide from Abcam (Cambridge, UK), and [^{125}I]-orexin-A from PerkinElmer (PerkinElmer Life and Analytical Sciences, Waltham, MA). Probenecid was from Sigma-Aldrich (St. Luis, MO), and

41 (SB-334867), i.e. *N*-biphenyl-2-yl-1-[[(1-methyl-1*H*-benzimidazol-2-yl)sulfanyl]acetyl]-L-prolinamide and **42** (TCS-1102), i.e. *N*-(2-methyl-6-benzoxazolyl)-*N'*-1,5-naphthyridin-4-yl urea from Tocris Bioscience (Bristol, UK).

Cell culture and Media. CHO-hOX$_1$ and -hOX$_2$ cells,[31,37] and control CHO-K1 cells (not expressing orexin receptors; control CHO cells), were cultured in Ham's F12 medium (Gibco/Life Technologies, Paisley, UK) + supplements on plastic cell culture dishes (56 cm^2 bottom area; Greiner Bio-One GmbH, Frickenhausen, Germany) as described in Jäntti et al. 2012.[33] For binding assay we used white and for Ca^{2+} measurements black clear-bottom half-area Cellstar µClear 96-well cell culture plates (Greiner Bio-One GmbH; Frickenhausen, Germany) with polyethyleneimine (25 µg/mL for 1 h at 37 °C; Sigma-Aldrich, St. Louis, MO, USA) coating. Hepes-buffered medium (HBM; 137 mM NaCl, 5 mM KCl, 1.2 mM MgCl$_2$, 0.44 mM KH$_2$PO$_4$, 4.2 mM NaHCO$_3$, 1 mM CaCl$_2$, 10 mM glucose, 20 mM HEPES and 0.1% (w/v) stripped bovine serum albumin, and adjusted to pH 7.4 with NaOH) was used as the basic experimental medium.

[^{125}I]-Orexin-A Competition Binding. We assessed the binding of the test compounds in intact cells essentially as in Turku et al. 2016.[9] The cells (1.5×10^4 per well) were plated on white clear bottom half-area 96-well plates. After 24h, the culture medium was exchanged for HBM + 30 µM dyngo 4a ± 10 µM **42** (to determine nonspecific binding). [^{125}I]-orexin-A / orexin-A mixture (at final concentration of 1 nM; 1:20) mixed with each test compound was added after 10 min of incubation. As controls we used dilution series of orexin-A and **41**. The plates were incubated for 90 min at room temperature, and then the medium was removed by water suction and the wells were allowed to dry. After adding the scintillation cocktail (Ultima Gold; PerkinElmer) the plates were counted in a Wallac Microbeta Trilux microplate liquid scintillation counter (PerkinElmer). Each ligand was tested 3–4 times at 10 µM in quadruplicate.

Ca^{2+} elevation. Ca^{2+} elevations were measured essentially as described before.[9,10] The cells, 1.5×10^4 per well, were plated on black, clear bottom half-area 96-well plates. Twenty-four hours later, cell culture medium was removed and the cells were loaded with the loading solution composed of FLIPR Calcium 4 Assay Kit (Molecular Devices, Sunnyvale, CA) dissolved in and diluted with HBM + 1 mM probenecid, for 60 min at 37 °C. Then, the plate was placed in a FlexStation 3 fluorescence plate reader (Molecular Devices) and the intracellular Ca^{2+} levels were measured as fluorescence changes (excitation at 485 nm, emission at 525 nm) at 37 °C. Each well was measured for 150 s with 30 s of baseline before compound addition. For K_i measurements, the test compounds (at concentrations 1–30 µM in a 5-fold dilution series) were added in the wells by FlexStation as a first addition, and the plate was measured once as described above. Then, 30 min later, 0.3 nM orexin-A was added as a stimulant and the measurement was repeated. K_i measurements were conducted in quadruplicate 3–4 times.

For agonist activity instead, antagonists **41** and **42** were added to wells manually, when applicable, and incubated for 30 min before the measurement, after which the test compounds were added by FlexStation, and the plate was measured only once. For potentiation studies the orexin-A / compound and ATP / compound mixtures were added by FlexStation as a first

addition, and then the plate was measured according to the agonist screen. For the agonist screen, the measurements were conducted in triplicate two individual times. The validation of the putative agonists **6**, **7** and **27**, and all potentiation studies were conducted in triplicate 3–4 individual times.

Data analysis. All data are presented as mean ± SEM. Microsoft Excel was used for data visualizations and analyses including curve fitting as described in Kukkonen 2016.[29] K_i values were calculated from the determined IC_{50} values using the Cheng−Prusoff equation.[38] Two highest concentrations (18 µM and 30 µM) were left out from the curve fitting due to the possibility of the nonspecific effects caused by the higher compound concentrations (e.g. colloidal aggregation, see below). Student's paired two-tailed t-test was used for the statistical comparisons. Significances are as follows: ns (not significant), $P > 0.05$; *$P < 0.05$; **$P < 0.01$; ***$P < 0.001$.

4.4 Aggregation. Compounds **19**, **22** and **32** were tested for colloidal aggregation in HBM using a Npheloskan Ascent (Labsystems, Finland). Compounds **19** and **32** were tested at concentrations 30 µM, 10 µM and 1 µM, and showed no aggregation at any of these concentrations (Supporting Information Figure S8, for further verification see Supporting Information Figure S9). Compound **22**, instead, was measured at 30 µM, 18 µM, 10 µM and 1 µM concentrations, of which the two highest showed some aggregate formation.

ASSOCIATED CONTENT

Supporting Information. R-groups used for constructing the virtual library (Figure 1), R-group analysis (Figures 2–3), IC_{50} curves (Figure 4), Structures of **41** (SB-334867) and **42** (TCS-1102) (Figure 5), Potentiation (Figures 6–7), Selecting the screening protocol, Aggregation (Figure 8–9), NMR spectra of compounds **6–25** and **27–31** (PDF).

AUTHOR INFORMATION

Corresponding Author
*E-mail: teppo.leino@helsinki.fi (T.O.L.)

Author Contributions
E.A.A.W., T.O.L and A.T outlined the initial idea of the study. A.T. designed, conducted and analyzed the computational part with H.X. T.O.L. designed the syntheses together with E.A.A.W and J.Y.-K., and synthesized the compounds. A.T. and J.P.K. designed, conducted and analyzed the pharmacological part of the study. A.T. and T.O.L. wrote the manuscript in collaboration with all co-authors. #T.O.L and A.T. contributed equally.

REFERENCES

[1]   T. Sakurai, A. Amemiya, M. Ishii, I. Matsuzaki, R. Chemelli, H. Tanaka, S. Williams, J. Richardson, G. Kozlowski, S. Wilson, J. Arch, R. Buckingham, A. Haynes, S. Carr, R. Annan, D. McNulty, W.-S. Liu, J. Terret, N. Elshourbagy, D. Bergsma, M. Yanagisawa, Orexins and orexin receptors: a family of hypothalamic neuropeptides and G protein-coupled receptors that regulate feeding behavior, Cell. 92 (1998) 573–585.

[2]   L. de Lecea, T.S. Kilduff, C. Peyron, X.-B. Gao, P.E. Foye, P.E. Danielsson, C. Fukuhara, E.L.F. Battenberg, V.T. Gautvik, F.S. Bartlett II, W.N. Frankel, A.N. Van Den Pol, F.E. Bloom, K.M. Gautvik, J.G. Sutcliffe, The hypocretins : Hypothalamus-specific peptides with neuroexcitatory activity, Proc. Natl. Acad. Sci. 95 (1998) 322–327.

[3]   A.J. Roecker, C.D. Cox, P.J. Coleman, Orexin Receptor Antagonists: New Therapeutic Agents for the Treatment of Insomnia, J. Med. Chem. 59 (2016) 504–530. doi:10.1021/acs.jmedchem.5b00832.

[4]   Q. Chen, L. De Lecea, Z. Hu, D. Gao, The Hypocretin / Orexin System : An Increasingly Important Role in Neuropsychiatry, Med. Res. Rev. 35 (2015) 152–197. doi:10.1002/med.

[5]   C. Boss, C. Roch, Expert Opinion on Therapeutic Patents Orexin research : patent news from 2016 Orexin research : patent news from 2016, Expert Opin. Ther. Pat. (2017) 1–11. doi:10.1080/13543776.2017.1344221.

[6]   M. Yanagisawa, Small-molecule Agonist for type-2 Orexin Receptor, Patent US20100150840A1, 2010.

[7]   M. Cano, P.M. Grima, A. Palomer Benet, 2-(2-aminophenoxy)-3-chloronaphthalene-1,4-dione Compounds Having Orexin 2 Receptor Agonist Activity, Patent WO2014198880, 2014.

[8]   T. Nagahara, T. Saitoh, N. Kutsumura, Y. Irukayama-Tomobe, Y. Ogawa, D. Kuroda, H. Gouda, H. Kumagai, H. Fujii, M. Yanagisawa, H. Nagase, Design and Synthesis of Non-Peptide, Selective Orexin Receptor 2 Agonists, J. Med. Chem. 58 (2015) 7931–7937. doi:10.1021/acs.jmedchem.5b00988.

[9]   A. Turku, A. Borrel, T.O. Leino, L. Karhu, J.P. Kukkonen, H. Xhaard, Pharmacophore Model To Discover OX1 and OX2 Orexin Receptor Ligands, J. Med. Chem. 59 (2016) 8263–8275. doi:10.1021/acs.jmedchem.6b00333.

[10] A. Turku, M.K. Rinne, G. Boije af Gennäs, H. Xhaard, D. Lindholm, J.P. Kukkonen, Orexin receptor agonist Yan 7874 is a weak agonist of orexin/hypocretin receptors and shows orexin receptor-independent cytotoxicity, PLoS One. 12 (2017) e0178526.

[11] A.L. Gotter, A.J. Roecker, R. Hargreaves, P.J. Coleman, C.J. Winrow, J.J. Renger, Orexin receptors as therapeutic drug targets, Prog. Brain Res. 198 (2012) 163–196.

[12] M. Laburthe, T. Voisin, The orexin receptor OX1R in colon cancer: a promising therapeutic target and a new paradigm in G protein-coupled receptor signalling through ITIMs., Br. J. Pharmacol. 165 (2012) 1678–87. doi:10.1111/j.1476-5381.2011.01510.x.

[13] J. Lee, M.M. Reddy, T. Kodadek, Discovery of an orexin receptor positive potentiator, Chem. Sci. 1 (2010) 48–54. doi:10.1039/c0sc00197j.

[14] G. Anderson, B. Steckler, Azulene. VIII. A Study of the Visible Absorption Spectra and Dipole Moments of Some 1- and 1,3-Substituted Azulenes, J. Am. Chem. Soc. 81 (1959) 4941–4946.

[15] T. Yanagisawa, S. Wakabayashi, T. Tomiyama, M. Yasunami, K. Takase, Synthesis and Anti-ulcer Activities of Sodium Alkylazulene Sulfonates, Chem. Pharm. Bull. 36 (1988) 641–647.

[16] A. Asato, A. Peng, M. Hossain, T. Mirzadegan, J.S. Bertramf, Azulenic Retinoids: Novel Nonbenzenoid Aromatic Retinoids with Anticancer Activity, J. Med. Chem. 36 (1993) 3137–3147.

[17] C. Chen, O. Lee, C. Yao, M. Chuang, Y. Chang, M. Chang, Y. Wen, W. Yang, C. Ko, N. Chou, M. Lin, C. Lai, C. Sun, L. Wang, Y. Chen, T. Hseu, C. Chang, H. Hsu, H. Lin, Y. Chang, Y. Shih, S. Chou, Y. Hsu, H. Tseng, C. Liu, C. Tu, T. Hu, Y. Tsai, T. Chen, C. Lin, S. Chiou, C. Liu, C. Hwang, Novel azulene-based derivatives as potent multi-receptor tyrosine kinase inhibitors, Bioorg. Med. Chem. Lett. 20 (2010) 6129–6132. doi:10.1016/j.bmcl.2010.08.025.

[18] B.-C. Hong, Y.-F. Jiang, E.S. Kumar, Microwave-Assisted [6+4]-Cycloaddition of Fulvenes and alpha-Pyrones to Azulene − Indoles : Facile Syntheses of Novel Antineoplastic Agents, Bioorg. Med. Chem. Lett. 11 (2001) 1981–1984.

[19] K. Ikegai, M. Imamura, T. Suzuki, K. Nakanishi, T. Murakami, E. Kurosaki, A. Noda, Y. Kobayashi, M. Yokota, T. Koide, K. Kosakai, Y. Ohkura, M. Takeuchi, H. Tomiyama, M. Ohta, Synthesis and biological evaluation of C-glucosides with azulene rings as selective SGLT2 inhibitors for the treatment of type 2 diabetes mellitus : Discovery of YM543, Bioorg. Med. Chem. 21 (2013) 3934–3948. doi:10.1016/j.bmc.2013.03.067.

[20] S. Löber, H. Hübner, A. Buschauer, F. Sanna, A. Argiolas, M.R. Melis, P. Gmeiner, Novel azulene derivatives for the treatment of erectile dysfunction, Bioorg. Med. Chem. Lett. 22 (2012) 7151–7154. doi:https://doi.org/10.1016/j.bmcl.2012.09.064.

[21] T.O. Leino, M. Baumann, J. Yli-Kauhaluoma, I.R. Baxendale, E.A.A. Wallén, Synthesis of 1,3,6-Trisubstituted Azulenes, J. Org. Chem. 80 (2015) 11513–11520. doi:10.1021/acs.joc.5b02271.

[22] T.O. Leino, L. Devisscher, N. Sipari, J. Yli-Kauhaluoma, E.A.A. Wallén, Synthesis of 1,3,6-Trisubstituted Azulenes Based on the 1-Acyloxyazulene Scaffold, Eur. J. Org. Chem. (2016) 5539–5544. doi:10.1002/ejoc.201600962.

[23] Schrödinger, Small-Molecule Drug Discovery Suite 2015-3: Schrödinger Suite 2015-3 Induced Fit Docking protocol; Glide version 6.8; Prime version 4.1, (2015).

[24] J. Yin, J.C. Mobarec, P. Kolb, D.M. Rosenbaum, Crystal structure of the human OX2 orexin receptor bound to the insomnia drug suvorexant, Nature. 519 (2015) 247–250. doi:10.1038/nature14035.

[25] J. Ballesteros, H. Weinstein, Integrated methods for the construction of three-dimensional models and computational probing of structure-function relations in G protein-coupled receptors, Methods Neurosci. 25 (1995) 366–428. doi:10.1016/S1043-9471(05)80049-7.

[26] H. Xhaard, T. Nyrönen, V.V. Rantanen, J.O. Ruuskanen, J. Laurila, T. Salminen, M. Scheinin, M.S. Johnson, Model structures of α-2 adrenoceptors in complex with automatically docked antagonist ligands raise the possibility of interactions dissimilar from agonist ligands, J. Struct. Biol. 150 (2005) 126–143. doi:10.1016/j.jsb.2004.12.008.

[27] L. Karhu, A. Turku, H. Xhaard, Modeling of the OX1R–orexin-A complex suggests two alternative binding modes, BMC Struct. Biol. 15 (2015) 1–17. doi:10.1186/s12900-015-0036-2.

[28] B.R. Travis, M. Sivakumar, G.O. Hollist, B. Borhan, Facile Oxidation of Aldehydes to Acids and Esters with Oxone, Org. Lett. 5 (2003) 1031–1034.

[29] J.P. Kukkonen, OX2 orexin/hypocretin receptor signal transduction in recombinant Chinese hamster ovary cells, Cell. Signal. 28 (2016) 51–60. doi:10.1016/j.cellsig.2015.11.009.

[30] J. Putula, T. Pihlajamaa, J.P. Kukkonen, Calcium affects OX1 orexin (hypocretin) receptor responses by modifying both orexin binding and the signal transduction machinery, Br. J. Pharmacol. 171 (2014) 5816–5828. doi:10.1111/bph.12883.

[31] P.E. Lund, R. Shariatmadari, A. Uustare, M. Detheux, M. Parmentier, J.P. Kukkonen, K.E.O. Åkerman, The orexin OX1 receptor activates a novel Ca2+ influx pathway necessary for coupling to phospholipase C, J. Biol. Chem. 275 (2000) 30806–30812. doi:10.1074/jbc.M002603200.

[32] S. Ammoun, L. Johansson, M.E. Ekholm, T. Holmqvist, A.S. Danis, L. Korhonen, O.A. Sergeeva, H.L. Haas, K.E.O. Åkerman, J.P. Kukkonen, OX1 Orexin Receptors Activate Extracellular Signal- Regulated Kinase in Chinese Hamster Ovary Cells via Multiple Mechanisms : The Role of Ca2+ Influx in OX1 Receptor Signaling, Mol. Endocrinol. 20 (2006) 80–99. doi:10.1210/me.2004-0389.

[33] M.H. Jäntti, J. Putula, P. Somerharju, M. Frohman, J.P. Kukkonen, OX1 orexin/hypocretin receptor activation of phospholipase D., Br. J. Pharmacol. 165 (2012) 1109–23. doi:10.1111/j.1476-5381.2011.01565.x.

[34] P.M. Turunen, M.H. Jantti, J.P. Kukkonen, OX1 orexin/hypocretin receptor signaling through arachidonic acid and endocannabinoid release, Mol Pharmacol. 82 (2012) 156–167. doi:10.1124/mol.112.078063.

[35] A. Turku, A. Borrel, T.O. Leino, L. Karhu, J.P. Kukkonen, H. Xhaard, Pharmacophore Model to Discover OX1 and OX2 Orexin Receptor Ligands, J. Med. Chem. 59 (2016). doi:10.1021/acs.jmedchem.6b00333.

[36] Schrödinger, Small-Molecule Drug Discovery Suite 2015-1: Schrödinger Suite 2015-1 Induced Fit Docking protocol; Glide version 6.6; Prime version 3.9, (2015).

[37] S. Ammoun, T. Holmqvist, R. Shariatmadari, H.B. Oonk, M. Detheux, M. Parmentier, K.E.O. Åkerman, J.P. Kukkonen, Distinct Recognition of OX1 and OX2 Receptors by Orexin Peptides, J. Pharmacol. Exp. Ther. 305 (2003) 507–514. doi:10.1124/jpet.102.048025.and.

[38] Y.-C. Cheng, W.H. Prusoff, Relationship between the inhibition constant (Ki) and the concentration of inhibitor which causes 50 per cent inhibition (I50) of an enzymatic reaction, Biochem. Pharmacol. 22 (1973) 3099–3108. doi:10.1016/0006-2952(73)90196-2.